

# Chapter 8

## Development of a Microreactor for Synthesis of $^{18}\text{F}$ -Labeled Positron Emission Tomography Probe

Norihito Kuno, Naomi Manri, Norifumi Abo, Yukako Asano, Ken-ichi Nishijima, Nagara Tamaki, and Yuji Kuge

**Abstract** *Background:* The application of microreactors to positron emission tomography (PET) probe radiosynthesis has attracted a great deal of interest because of its potential to increase specific activity and yields of probes and to reduce reaction time, expensive reagent consumption, and the footprint of the device/instrument. To develop a microreactor platform that enables the synthesis of various  $^{18}\text{F}$ -labeled PET probes, a prototype microreactor with a novel “split-flow and interflow mixing” (split mixing) was fabricated and applied to  $^{18}\text{F}$ -labeling reactions.

*Methods:* The split mixing microreactor, made of  $\text{Al}_2\text{O}_3$  resistant to several solvents, had higher mixing performance than that of the conventional batch

---

N. Kuno (✉)

Center for Exploratory Research, Research and Development Group, Hitachi, Ltd., 1-280, Higashi-koigakubo, Kokubunji, Tokyo 185-8601, Japan  
e-mail: [norihito.kuno.py@hitachi.com](mailto:norihito.kuno.py@hitachi.com)

N. Manri

Center for Technology Innovation – Healthcare, Research and Development Group, Hitachi, Ltd., 1-280, Higashi-koigakubo, Kokubunji, Tokyo 185-8601, Japan  
e-mail: [naomi.manri.hd@hitachi.com](mailto:naomi.manri.hd@hitachi.com)

N. Abo • K. Nishijima

Central Institute of Isotope Science, Hokkaido University, Kita 15 Nishi 7, Kita-ku, Sapporo 060-0815, Japan  
e-mail: [abo@ric.hokudai.ac.jp](mailto:abo@ric.hokudai.ac.jp); [nishijim@ric.hokudai.ac.jp](mailto:nishijim@ric.hokudai.ac.jp)

Y. Asano

Center for Technology Innovation – Mechanical Systems, Research and Development Group, Hitachi, Ltd., 832-2 Horiguchi, Hitachinaka, Ibaraki 312-0034, Tokyo, Japan  
e-mail: [yukako.asano.dp@hitachi.com](mailto:yukako.asano.dp@hitachi.com)

N. Tamaki

Department of Nuclear Medicine, Graduate School of Medicine, Hokkaido University, Sapporo, Japan  
e-mail: [natamaki@med.hokudai.ac.jp](mailto:natamaki@med.hokudai.ac.jp)

Y. Kuge

Central Institute of Isotope Science, Hokkaido University Department of Integrated Molecular Imaging, Graduate School of Medicine, Hokkaido University, Sapporo, Japan  
e-mail: [kuge@ric.hokudai.ac.jp](mailto:kuge@ric.hokudai.ac.jp)

method. Two  $^{18}\text{F}$ -labeling reactions ( $^{18}\text{F}$  labeling of bovine serum albumin (BSA) by N-succinimidyl-4- $^{18}\text{F}$  fluorobenzoate (SFB) and 1-(2'-nitro-1'-imidazolyl)-2-O-tetrahydropyranyl-3-O-toluenesulfonylpropanediol (NITTP) by  $^{18}\text{F}$ ) were conducted using the microreactor.

*Results:* The  $^{18}\text{F}$ -labeling yield of BSA obtained by using the microreactor was almost the same as that by using the conventional batch method; however, the reaction time of the microreactor was slightly shorter than that of the batch method. Conversely, the  $^{18}\text{F}$ -labeling yield of NITTP obtained by using the microreactor was about half that by using the batch method. The low NITTP-labeling yield was due to adsorption of naked  $^{18}\text{F}$  to the surface of micro-mixing channel in the microreactor. The prescreening of candidate materials with lower  $^{18}\text{F}$  adsorption for the microreactor was carried out with solvent resistance and solvent absorption as indexes. As a result of this prescreening, cyclo olefin polymer (COP) was selected as a candidate. A prototype COP microreactor has been fabricated and is being evaluated in terms of  $^{18}\text{F}$  labeling.

*Conclusions:* Although the higher mixing performance of the split mixing microreactor did not significantly contribute to increasing  $^{18}\text{F}$ -labeling yield, it did contribute to shortening reaction time. Moreover, the material used for the microreactor should be carefully selected from the viewpoint of developing a microreactor platform that enables the synthesis of various  $^{18}\text{F}$ -labeled PET probes.

**Keywords** Positron emission tomography (PET) • Microreactor •  $^{18}\text{F}$ -labeled PET probe • Cyclo olefin polymer (COP)

## 8.1 Introduction

Positron emission tomography (PET) is a noninvasive, nuclear imaging technique that has been widely applied for medical research and clinical diagnosis in the fields of oncology, neurology, and cardiology [1–4]. PET imaging relies on the utilization of a PET probe labeled with short-lived positron-emitting radioisotopes such as  $^{11}\text{C}$  ( $t_{1/2} = 20$  min) or  $^{18}\text{F}$  ( $t_{1/2} = 110$  min). Among several PET probes, 2- $^{18}\text{F}$ -fluoro-2-deoxy-d-glucose ( $^{18}\text{F}$ -FDG), an analog of glucose, is most commonly used in the diagnosis and assessment of cancer. Moreover, utilized in clinical oncology, it shows excellent performance as a PET imaging probe [5].

$^{18}\text{F}$ -FDG has been extensively utilized as the PET imaging probe in oncologic application. However, in the last few decades, a large number of non-FDG PET probes have been developed to measure and elucidate various biological and physiological processes [6, 7].

With the increasing variation of PET probes that are applicable to clinical diagnosis, for diagnosis of individual patients, it is necessary to produce a wide variety of PET probes in small quantities. It is therefore also necessary to modify the supply system for PET probe (such as a centralized mass production) and the commercial delivery system that were established for a single PET probe, i.e.,  $^{18}\text{F}$ -FDG [8].

Meanwhile, decentralized, in-house production of PET probes also has some difficulties in regard to the production of a wide variety of PET probes in small quantities, because of the need for a large investment in infrastructure in accordance with government regulations, an expensive “hot cell” for radiation shielding of PET probe synthesizer, and high personnel and operating costs. Moreover, the number of synthesizer that can be installed in a hot cell is restricted because of the limited workspace in the hot cell; accordingly, it is difficult to accomplish in-house small-scale production of multiple PET probes.

Recently, to solve the abovementioned problems concerning small-scale production of various PET probes, the application of microreactors (or microfluidic devices) to the PET probe radiosynthesis has attracted a great deal of interest because of their potential to increase specific activity and yields of the probes and to reduce reaction time, consumption of expensive reagents, and footprint of the device/instrument [9, 10].

Microreactor can be categorized as flow-through type or batch type. And both a flow-through microreactor and a batch microreactor have been applied to radiosynthesis of PET probes for  $^{18}\text{F}$  labeling [11]. Almost all previous studies on applying microreactors for radiosynthesis of PET probes have been limited to preclinical PET imaging; however, a few recent studies attempted to apply microreactors for synthesizing the clinical PET probes such as  $^{18}\text{F}$ -fallypride, the dopamine D2/D3 receptors imaging probe [12]; 7-(6-fluoropyridin-3-yl)-5H-pyrido [4,3-b]indole ( $^{18}\text{F}$ -T807), tau imaging probe [13]; and  $^{18}\text{F}$ -labeled 3-fluoro-5-[(pyridin-3-yl)ethynyl]benzotrile ( $^{18}\text{F}$ -FPFB), the glutamate receptor subtype type 5 (mGluR5) imaging probe [14].

Moreover, a microreactor for radiosynthesis of a clinical PET probe has not been applied as the routine production method for clinical usage. It is still a great challenge to solve several problems hindering the practical use of microreactors for synthesizing PET imaging probes for clinical applications.

In a previous study, microreactor systems with novel mixing methods were established and applied to achieve large-scale and industrial production of chemicals [15, 16]. In this study, a prototype microreactor with a novel split-flow and interflow mixing (called “split mixing”) was fabricated and evaluated in regard to  $^{18}\text{F}$ -labeling reactions.

## 8.2 Materials and Methods

### 8.2.1 Villiermaux-Dushman Method

The mixing performance of the prototype microreactor was evaluated by Villiermaux-Dushman method [17]. Solution X (HCl: 0.1374 M) and solution Y (KI, 0.01595 M;  $\text{CH}_3\text{COONa}$ , 1.33 M;  $\text{KIO}_3$ , 0.003175 M) were separately supplied to the microreactor by Micro Process Server (MPS- $\alpha$ 200, Hitachi, Tokyo,

Japan). The solution mixed in the microreactor was collected and left for two minutes. The flow rate of the two solutions was set at 0.2, 0.5, 1.0, 2.0, 4.0, and 6.0 mL/min. Absorbance at 350 nm was measured by a UV-visible spectrometer (U-3010, Hitachi-High Technologies, Tokyo, Japan).

### 8.2.2 $^{18}\text{F}$ Labeling of BSA by $^{18}\text{F}$ -SFB

Succinimidyl-4- $^{18}\text{F}$ fluorobenzoate ( $^{18}\text{F}$ -SFB) was synthesized by a method similar to that reported by Tang et al. [18]. The synthesized  $^{18}\text{F}$ -SFB was evaporated at 100 °C under an argon stream and dissolved in 20 % acetonitrile (MeCN) (0.3 MBq/ $\mu\text{L}$ ). Bovine serum albumin (BSA) dissolved in 125 mM borate buffer (pH8.8) (5 mg/mL) was used as a target protein. By the microreactor method,  $^{18}\text{F}$ -SFB and BSA solutions were separately injected into the microreactor by using the MPS- $\alpha$ 200. The mixed solution was introduced into a PTFE tube ( $\phi$ 0.17  $\times$  250 mm, GL science, Tokyo, Japan) connected to an outlet of the microreactor. The reaction mixture was collected at times of 2, 10, and 20 min by driving the MPS- $\alpha$ 200, and TFA was added to the reaction mixture to terminate the reaction. By the conventional batch method, the  $^{18}\text{F}$ -SFB and BSA solutions were mixed in equal amount at room temperature in a 1.5 mL microtube. Trifluoroacetic acid (TFA) was added to the mixture to terminate the reaction at times of 2, 10, and 20 min.

LC analysis was performed using a Nexera X2 UHPLC/HPLC system (Shimadzu, Kyoto, Japan). The reaction mixture (20  $\mu\text{L}$ ) was loaded onto a C8 reversed-phase column (CAPCELL PAK C8 SG300, Shiseido, Tokyo, Japan). The LC solvents were (A) 2 % MeCN/0.05 % TFA and (B) 80 % MeCN/0.05 % TFA, and a gradient (40 % B: 0–1.5 min, 100 % B: 1.5–2.5 min, 40 % B: 2.5–9.0 min) was used at a flow rate of 0.3 mL/min. The percentage of  $^{18}\text{F}$ -benzoic acid ( $^{18}\text{F}$ -FBzA),  $^{18}\text{F}$ -SFB, and  $^{18}\text{F}$ -BSA was calculated from the LC data.

### 8.2.3 $^{18}\text{F}$ Labeling of NITTP by $^{18}\text{F}$

An aqueous solution of  $^{18}\text{F}^-$ , produced by cyclotron using the  $^{18}\text{O}$  (p, n)  $^{18}\text{F}$  reaction, was passed through a Sep-Pak Light QMA cartridge (Waters Corporation, MA, USA). The  $^{18}\text{F}$  activity was eluted with a 0.9 mL (0.7 mL MeCN/0.2 mL water) solution containing 14 mg Kryptofix222 (K222) and 1.4 mg  $\text{K}_2\text{CO}_3$ . The eluent was then evaporated at 100 °C under an argon stream. The residue, containing  $[\text{K}/\text{K}222]^{+18}\text{F}^-$ , was dissolved in dimethyl sulfoxide (DMSO) (0.22 MBq/ $\mu\text{L}$ ).

1-(2'-Nitro-1'-imidazolyl)-2-O-tetrahydropyranyl-3-O-toluenesulfonyl-propanediol (NITTP, ABX GmbH, Radeberg, Germany) was dissolved in DMSO (1.3 mg/mL). By the microreactor method,  $[\text{K}/\text{K}222]^{+18}\text{F}^-$  and NITTP solutions

were separately sent to the microreactor by using a dual syringe pump (TSP-202, YMC, Kyoto, Japan). The solution mixed in the microreactor was then sent to a PTFE tube ( $\varnothing 0.5 \times 510$  mm, GL science) connected to an outlet of the microreactor, and the reaction in the PTFE tube was allowed to proceed for 3 or 10 min at 80 °C. By the batch method,  $[\text{K/K222}]^+{}^{18}\text{F}^-$  and NITTP solutions were mixed in equal amount in a 1.5 mL microtube. The reaction was allowed to proceed for 3 or 10 min at 80 °C. LC analysis was performed using a Nexera X2 (Shimadzu). The reaction mixture (10  $\mu\text{L}$ ) was loaded onto a C18 reversed-phase column (XBridge C18, 5  $\mu\text{m}$ , 4.6 mm  $\times$  150 mm, Waters Corporation). The LC solvents were (A) 50 mM  $(\text{NH}_4)_2\text{HPO}_4$  and (B) MeCN, and isocratic elution (45 % B) was used at a flow rate of 1 mL/min. Percentage of  ${}^{18}\text{F}$ -NITTP was calculated from the LC data.

### 8.2.4 Solvent Resistance Test

The chemical resistance of seven materials (polyvinyl chloride [PVC], polystyrene [PS], acrylonitrile-butadiene-styrene resin [ABS], methacrylate resin [PMMA], polycarbonate [PC], polypropylene [PP], and cyclo olefin polymer [COP]) against five chemicals (acetonitrile [MeCN], dimethyl sulfoxide [DMSO], hydrochloric [HCl], sodium hydroxide [NaOH], and ethanol [EtOH]) was tested. A test piece (size: 10  $\times$  10  $\times$  t2 mm) was dropped into each of the chemicals set at 25, 50, 80, or 120 °C, and the reaction was allowed to proceed for 30 min. The condition of the test piece was observed, and the weight of the test piece was measured (W1) after the reaction was completed. After the test piece was washed with water, it was dehydrated for 24 h at 50 °C. The weight of the test piece was measured again (W2). The volume of the chemical absorbed in the test piece was calculated from the difference between W1 and W2.

## 8.3 Results and Discussion

### 8.3.1 Microreactor with Novel Mixing System

Two microreactors with different types of mixing, i.e., split-flow and interflow (“split mixing”) and multilayer channels contracting toward the downstream (“multimixing”), were fabricated (Fig. 8.1a, b). The split mixing microreactor was made of  $\text{Al}_2\text{O}_3$ , and the multimixing one was made of PEEK. Both materials,  $\text{Al}_2\text{O}_3$  and PEEK, were selected from the viewpoint of resistance to several solvents and fabricability of micro channel structure for mixing.

On the split mixing microreactor, the first liquid (solution A) and the second liquid (solution B) were injected into the micro channels of the microreactor. The

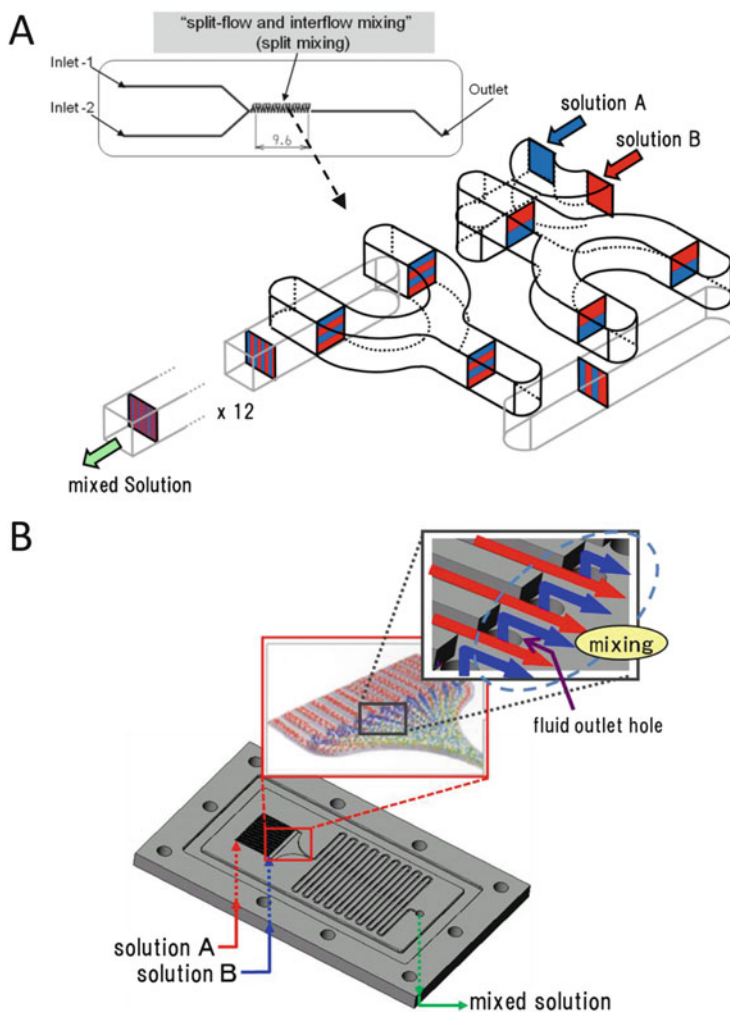


**Fig. 8.1** Schematics of microreactors used in this study. (a) The split-flow and interflow microreactor. The flow of fluids in the micro channel for mixing is shown in the cross section of the micro channel. (b) The multilayer channels contracting toward the downstream microreactor

parallel flow of two fluids (solutions A and B) was split, rotated 90° (inversion), and interflowed repeatedly (12 times) as the fluids pass through the repeated split mixing structures of the microreactor. Finally, the flow of two fluids formed an alternately multilayered thin flow of fluids (Fig. 8.1a). As the thickness of each fluid became small, the diffusion time of the reactants of fluids (solutions A and B) was reduced, causing faster mixing of the solutions.

On the multimixing microreactor, the first liquid (solution A) flows from each nozzle in layer form on top of the chip. In the center of the chip, the second liquid

(solution B) supplied from multi-outlet holes flows into the layered first liquid. Then, both fluids form a multilayered flow at a contraction flow part on the bottom of the chip to produce the thin flow of fluids (Fig. 8.1b).

### 8.3.2 Evaluation of Mixing Performance of Prototype Microreactors

Mixing performance of the prototype microreactors was evaluated by using the Villiermaux-Dushman method [17], shown in Fig. 8.2a. By this method, the side reaction product,  $I_3^-$ , was spectroscopically measured by using the mean of UV absorbance at 350 nm. Therefore, lower UV absorbance indicates higher mixing performance. The mixing performance of the split mixing microreactor was higher than that of the multimixing microreactor and that of a conventional batch method (Fig. 8.2b). From this result, the split mixing microreactor was selected for further analysis of  $^{18}F$ -labeling reaction.

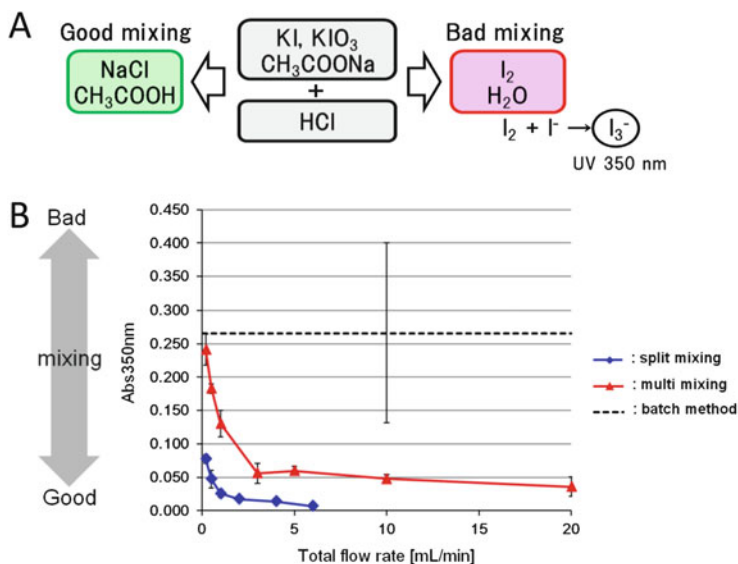


**Fig. 8.2** (a) Schematic of the Villiermaux-Dushman method. (b) Mixing performance of the split-flow and interflow (“split mixing”) microreactor ( $\diamond$ ) and the multilayer channels contracting toward the downstream (“multimixing”) microreactor ( $\Delta$ )

### 8.3.3 $^{18}\text{F}$ Labeling of Bovine Serum Albumin (BSA) by $N$ -succinimidyl-4- $^{18}\text{F}$ Fluorobenzoate ( $^{18}\text{F}$ -SFB)

The  $^{18}\text{F}$ -labeling reaction of BSA by  $^{18}\text{F}$ -SFB was examined to evaluate the  $^{18}\text{F}$ -labeling performance of the split mixing microreactor. This reaction consists of a main reaction ( $^{18}\text{F}$  labeling of BSA) and a side reaction which produce  $^{18}\text{F}$ -fluorobenzoic acid ( $^{18}\text{F}$ -FBzA) as a by-product (Fig. 8.3a).

As shown in Fig. 8.3b, the  $^{18}\text{F}$ -labeling yield of BSA obtained by using the split mixing microreactor was almost the same as that by using the conventional batch method (Fig. 8.3b). A by-product,  $^{18}\text{F}$ -FBzA, was synthesized in the same manner as that of batch method. These results suggest that as well as the main reaction, the side reaction is likely to proceed due to the higher mixing performance of the split mixing-type microreactor; therefore, the higher mixing performance might not be effective for increasing the  $^{18}\text{F}$ -labeling yield of BSA.

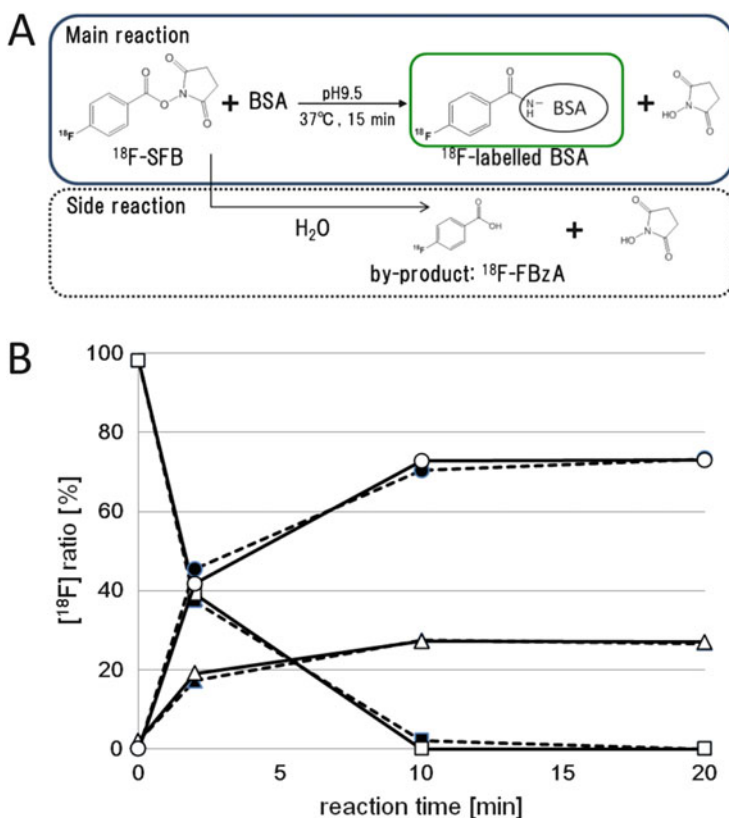


**Fig. 8.3** (a) Synthesis of  $^{18}\text{F}$ -labeled BSA by  $N$ -succinimidyl-4- $^{18}\text{F}$  fluorobenzoate ( $^{18}\text{F}$ -SFB). (b) Time courses of  $^{18}\text{F}$ -BSA ( $\circ$ ,  $\bullet$ ),  $^{18}\text{F}$ -FBzA ( $\triangle$ ,  $\blacktriangle$ ), and  $^{18}\text{F}$ -SFB ( $\diamond$ ,  $\blacklozenge$ ) synthesis of the split mixing microreactor (solid line) and the conventional batch method (broken line)



The reaction time of  $^{18}\text{F}$  labeling of BSA was estimated from a reaction rate constant calculated from the HPLC data. The estimated reaction time (10 min) for the  $^{18}\text{F}$  labeling of BSA by the microreactor method was shorter than that by the batch method (12 min). This result suggests that high mixing performance contributes to shortening the reaction time.

### 8.3.4 $^{18}\text{F}$ Labeling of 1-(2'-nitro-1'-imidazolyl)-2-O-tetrahydropyranyl-3-O-toluenesulfonylpropanediol (NITTP) by $^{18}\text{F}$

To further evaluate the  $^{18}\text{F}$ -labeling performance of the split mixing microreactor, the  $^{18}\text{F}$ -labeling reaction of NITTP was investigated (Fig. 8.4a). NITTP is a precursor for the synthesis of  $^{18}\text{F}$ -fluoromisonidazole ( $^{18}\text{F}$ -FMISO), which is a PET imaging probe for determining the tumor hypoxia in vivo [19].

The  $^{18}\text{F}$ -labeling yield of NITTP (at reaction time of 10 min) obtained by using the microreactor was 26 %, which is about half of that by using the batch method (59 %) (Fig. 8.4b). By measuring the total  $^{18}\text{F}$  activity of all solutions applied for the microreactor reaction, only 65 % of the initial  $^{18}\text{F}$  activity was recovered, and about 20 % of that was remained in the micro channels of microreactor. This result suggests that the low NITTP-labeling yield is due to adsorption of naked  $^{18}\text{F}$  to the

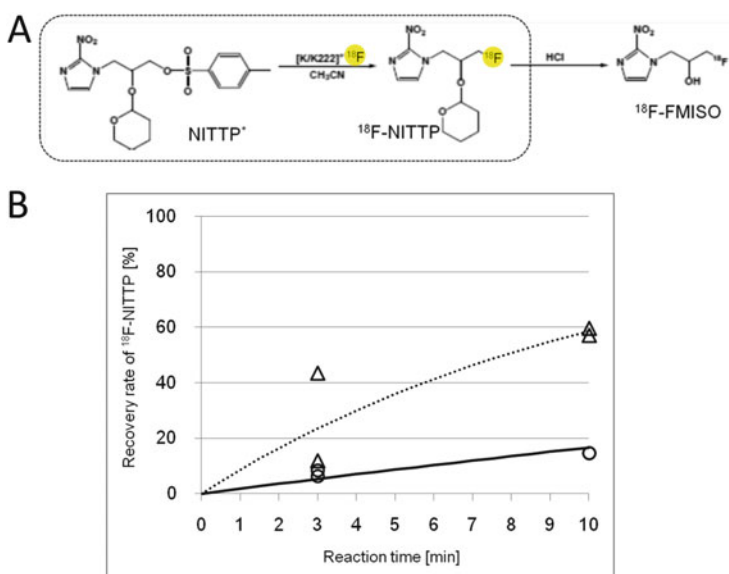


**Fig. 8.4** (a) Synthesis of  $^{18}\text{F}$ -NITTP and  $^{18}\text{F}$ -FMISO. (b) Time courses of  $^{18}\text{F}$ -NITTP synthesis of the split mixing microreactor (O, solid line) and the conventional batch method ( $\Delta$ , broken line)

surface of micro channels. To improve the  $^{18}\text{F}$ -labeling yield of NITTP attained by naked  $^{18}\text{F}$ , the material used for the microreactor should be reexamined.

### 8.3.5 Screening of Material for the Split Mixing Microreactor

As a first step of selecting the material for the microreactor, prescreening of candidate materials was carried out with solvent resistance and solvent absorption as indexes. The solvent resistance and absorption of seven kinds of materials, namely, polyvinyl chloride (PVC), polystyrene (PS), acrylonitrile-butadiene-styrene resin (ABS), methacrylate resin (PMMA), polycarbonate (PC), polypropylene (PP), and cyclo olefin polymer (COP), were tested for acetonitrile (MeCN), dimethyl sulfoxide (DMSO), hydrochloric acid (HCl), sodium hydroxide (NaOH), and ethanol (EtOH) at 25, 50, and 80 °C. Among these materials, PP and COP exhibited relatively better solvent resistant and lower solvent absorption than other materials. PP and COP exhibited excellent solvent resistant and lower absorption for HCl, NaOH, and EtOH; however, at the higher temperature, PP showed a decrease of solvent resistant and COP showed little absorption of solvent (Table 8.1).

As a candidate material for the microreactor, COP was selected for the microreactor because of the higher solvent resistance at high temperature (80 °C) of COP. As a preliminary experiment, a prototype COP microreactor was fabricated, and the remaining  $^{18}\text{F}$  activity after passing a  $^{18}\text{F}$  containing solution through the micro channels of the COP microreactor was determined. The remaining  $^{18}\text{F}$  activity was about 5 % of total  $^{18}\text{F}$  activity injected into the microreactor, which is lower than that (35 %) in the case of  $\text{Al}_2\text{O}_3$  microreactor. This result indicates that the COP microreactor is applicable to efficient  $^{18}\text{F}$  labeling for PET imaging probe.

**Table 8.1** Solvent resistance and absorption test

	Temp (°C)	MeCN			DMSO		
		25	50	80	25	50	80
PP	Resistance	+	+	–	+	+	+
	Absorption( $\mu\text{l}$ )	<5	<5	5 ~ 10	<5	<5	<5
COP	Resistance	+	+	+	+	+	+
	Absorption( $\mu\text{l}$ )	<5	<5	<5	<5	5 ~ 10	5 ~ 10

+, resistance; –, nonresistance

## 8.4 Conclusion

Although the higher mixing performance of the microreactor did not significantly contribute to increasing the  $^{18}\text{F}$ -labeling yield, it did contribute to shortening the reaction time. Moreover, selecting the appropriate material for the microreactor is crucial from the viewpoint of developing a microreactor platform that enables the synthesis of various  $^{18}\text{F}$ -labeled PET probes.

**Acknowledgment** This work was supported in part by the Creation of Innovation Centers for Advanced Interdisciplinary Research Areas Program, Ministry of Education, Culture, Sports, Science and Technology, Japan.

**Open Access** This chapter is distributed under the terms of the Creative Commons Attribution-Noncommercial 2.5 License (<http://creativecommons.org/licenses/by-nc/2.5/>) which permits any noncommercial use, distribution, and reproduction in any medium, provided the original author(s) and source are credited.

The images or other third party material in this chapter are included in the work's Creative Commons license, unless indicated otherwise in the credit line; if such material is not included in the work's Creative Commons license and the respective action is not permitted by statutory regulation, users will need to obtain permission from the license holder to duplicate, adapt or reproduce the material.

## References

1. Phelps ME. Positron emission tomography provides molecular imaging of biological processes. *Proc Natl Acad Sci U S A*. 2000;97:9226–33.
2. Gambhir SS. Molecular imaging of cancer with positron emission tomography. *Nat Rev Cancer*. 2002;2:683–93.
3. Politis M, Piccini P. Positron emission tomography imaging in neurological disorders. *J Neurol*. 2012;259:1769–80.
4. Schindler TH, Schelbert HR, Quercioli A, Dilsizian V. Cardiac PET imaging for the detection and monitoring of coronary artery disease and microvascular health. *JACC Cardiovasc Imaging*. 2010;3:623–40.
5. Otsuka H, Graham M, Kubo A, Nishitani H. Clinical utility of FDG PET. *J Med Invest*. 2004;51:14–9.
6. Brower V. Beyond FDG: many molecular imaging agents are in development. *J Natl Cancer Inst*. 2011;103:13–5.
7. The Radiosynthesis Database of PET Probes (RaDaP). National Institute of Radiological Sciences, Japan. 2013. <http://www.nirs.go.jp/research/division/mic/db2/>
8. Keng PY, Esterby M, van Dam RM. Emerging technologies for decentralized production of PET tracers. In: Hsieh CH, editor. *Positron emission tomography – current clinical and research aspects*. Rijeka: InTech; 2012. p. 53–182.
9. Lu SY, Pike VW. Micro-reactors for PET tracer labeling. In: Schubiger PA, Lehmann L, Friebe M, editors. *PET chemistry*. Berlin: Springer; 2007. p. 271–87.
10. Pascali G, Watts P, Salvadori PA. Microfluidics in radiopharmaceutical chemistry. *Nucl Med Biol*. 2013;40:776–87.
11. Elizarov AM. Microreactors for radiopharmaceutical synthesis. *Lab Chip*. 2009;9:1326–33.

12. Lebedev A, Miraghaie R, Kotta K, Ball CE, Zhang J, Buchsbaum MS, Kolb HC, Elizarov A. Batch-reactor microfluidic device: first human use of a microfluidically produced PET radiotracer. *Lab Chip*. 2013;13:136–45.
13. Liang SH, Yokell DL, Normandin MD, Rice PA, Jackson RN, Shoup TM, Brady TJ, El Fakhri G, Collier TL, Vasdev N. First human use of a radiopharmaceutical prepared by continuous-flow microfluidic radiofluorination: proof of concept with the tau imaging agent [<sup>18</sup>F]T807. *Mol Imaging* 2014;13. doi:[10.2310/7290.2014.00025](https://doi.org/10.2310/7290.2014.00025).
14. Liang SH, Yokell DL, Jackson RN, Rice PA, Callahan R, Johnson KA, Alagille D, Tamagnan G, Collier TL, Vasdev N. Microfluidic continuous-flow radiosynthesis of [<sup>18</sup>F]FPEB suitable for human PET imaging. *Medchemcomm*. 2014;5:432–5.
15. Asano Y, Togashi S, Tsudome H, Murakami S. Microreactor technology: innovations in production processes. *Pharm Eng*. 2010;8:32–42.
16. Asano Y, Miyamoto T, Togashi S, Endo Y. Study on the sandmeyer reaction via an unstable diazonium ion in microreactors with reaction rate analyses. *J Chem Eng Jpn*. 2014;47:287–95.
17. Ehrfeld W, Golbig K, Hessel V, Löwe H, Richter T. Characterization of mixing in micromixers by a test reaction: single mixing units and mixer arrays. *Ind Eng Chem Res*. 1999;38:1075–82.
18. Tang G, Zeng W, Yu M, Kabalka G. Facile synthesis of N-succinimidyl 4-[<sup>18</sup>F]fluorobenzoate ([<sup>18</sup>F]SFB) for protein labeling. *J Label Compd Radiopharm*. 2008;51:68–71.
19. Dubois L, Landuyt W, Haustermans K, Dupont P, Bormans G, Vermaelen P, Flamen P, Verbeken E, Mortelmans L. Evaluation of hypoxia in an experimental rat tumour model by [(18)F] fluoromisonidazole PET and immunohistochemistry. *Br J Cancer*. 2004;91:1947–54.